Available online at www.sciencedirect.com
SCIENCE DIRECT®
Journal of Solid State Chemistry 170 (2003) 75–81
JOURNAL OF SOLID STATE CHEMISTRY
http://elsevier.com/locate/jssc

Novel rare-earth borosilicide $RE_{1-x}B_{12}Si_{3.3-\delta}$ (RE = Y, Gd–Lu) ($0 \leqslant x \leqslant 0.5, \delta \approx 0.3$): synthesis, crystal growth, structure analysis and properties

F.X. Zhang,[a] F.F. Xu,[a] T. Mori,[a,b] Q.L. Liu,[a] and T. Tanaka[a,*]

[a] *Advanced Materials Laboratory, National Institute for Materials Science (NIMS), Namiki 1-1, Tsukuba, Ibaraki 305-0044, Japan*
[b] *PRESTO, Japan Science and Technology Corporation (JST), Japan*

Received 28 March 2002; received in revised form 21 June 2002; accepted 27 August 2002

Abstract

New rare-earth boron-rich compounds with the formula of $RE_{1-x}B_{12}Si_{3.3-\delta}$ (RE = Y, Gd–Lu) ($0 \leqslant x \leqslant 0.5, \delta \approx 0.3$) have been synthesized. They belong to a new type of rhombohedral structure with the space group of R-3m (No. 166) and $z = 9$. The lattice constants were measured from powder XRD data. Crystal structure solved from powder XRD data for $Tb_{0.68}B_{12}Si_3$ as a representative has been compared with that of $YB_{17.6}Si_{4.6}$ (or $Y_{0.68}B_{12}Si_{3.01}$), whose structure was solved from single-crystal reflection data. The structure model is confirmed by high-resolution transmission microscope analysis. The vibrational modes of the new crystals were measured by Raman spectroscopy. Temperature dependence of magnetic susceptibility which was measured for $RE_{1-x}B_{12}Si_{3.3-\delta}$ single crystals by SQUID revealed that they are paramagnetic materials down to 2.0 K.

Keywords: Boron-rich compound; Powder XRD; $RE_{1-x}B_{12}Si_{3.3-\delta}$; Structure refinement

1. Introduction

Boron-rich compounds have attracted much attention in the last two decades because of their unique crystal structure and interesting physical properties [1,2]. Many new rare-earth boron-rich solids have been found in the binary systems [3,4] and RE–B–C ternary systems [5–8] in recent years. Boron atoms in these compounds form rigid framework with interconnected stable clusters such as icosahedra and octahedra, etc., rare-earth elements reside in the voids of the framework. Due to the electron deficiency of the boron clusters, these rare-earth boron-rich compounds are usually semiconductors. Silicon is an element with strong covalent bonding tendency and many boron-rich compounds have been found in the Si–B system [9]. However, the phase behavior of RE–B–Si ternary systems, especially in boron-rich region was seldom studied till recently when a new ternary compound of $REB_{41}Si_{1.2}$, which is isostructural with YB_{50}, was found [10] during the crystal growth investigation of YB_{50} by the floating zone method. The ternary compound containing Tb in this series shows an antiferromagnetic transition at low temperature [11]. So the formation of new compounds and the investigation of their properties in the RE–B–Si systems is a quite new and interesting field. Very recently, another new type of boron-rich compound with composition of $YB_{17.6}Si_{4.6}$ (or $Y_{0.68}B_{12}Si_{3.01}$) was found in the Y–B–Si ternary system [12]. It was indexed with a rhombohedral structure with cell parameters of $a = b = 10.0841$ Å, $c = 16.4714$ Å and space group R-3m (No. 166) from single-crystal X-ray diffraction data. The boron atoms in the new structure form icosahedra, which stack along the c-axis forming boron icosahedral layer. Each icosahedron is interconnected with four neighbors within one layer. However, the boron icosahedra in different layers are not bonded directly and they are only linked through Si–Si bridges and Y atoms reside in the voids, which lie between boron icosahedral layers. Further investigations revealed that other rare-earth elements from Gd to Lu can also form the same structure. Here, we report on the structural analysis from powder X-ray diffraction

*Corresponding author.
E-mail address: tanaka.takaho@nims.go.jp (T. Tanaka).

0022-4596/03/$ - see front matter © 2002 Elsevier Science (USA). All rights reserved.
PII: S0022-4596(02)00025-7

pattern by the Rietveld method and high-resolution transmission electron microscope observations, single-crystal growth, vibrational and magnetic properties measurements for other *RE*–B–Si compounds.

2. Experimental

Powder samples were synthesized by solid state reaction with starting materials of REB_4, REB_6, SiB_6 and amorphous B (SB-Boron Inc., USA). REB_4 and REB_6 were obtained by the borothermal reduction method from the corresponding oxides, except the case of RE = Y, Tb and Er, for which commercial powders (YB_4 and TbB_6 (Japan New Metal Co. Ltd), ErB_4 (CERAC, USA)) were used. The details of the synthesis and purification process can be found in Refs. [3,12]. The solid-state reaction was performed at around 1650°C in an RF heating furnace with a BN crucible and a graphite susceptor under a vacuum environment. Single crystals were obtained by high-temperature solution growth method by using Si as the flux under a flowing argon atmosphere. Wet chemical analysis and EPMA analysis were performed to analyze the compositions of powders and single crystals, respectively.

The unit cell parameters were determined from powder XRD data with the program TREOR90 [13]. The powder X-ray diffraction profile of pure phase in the Tb–B–Si system was collected using a Rigaku RINT2200 powder X-ray diffactormeter with graphite-monochromated Cu$K\alpha$ radiation. The reflection data were collected from 5° to 130° with step width of 0.02° and recording time of 10 s for each step. The crystal structure was solved by using the program EXPO [14,15], a combination software of EXTRA and SIRPOW97, and finally refined by the Rietveld method with the program Fullprof [16]. A pseudo-Voigt profile function was used to describe the peaks shape during refinement.

TEM analysis was performed on a JEOL300 high-resolution transmission electron microscope. The compositions of the samples were analyzed by wet chemical method and the details are described in Ref. [10]. The Raman spectra of the single crystals were measured in a backscattering mode using the 514 nm line of an Ar ion laser at a spectral resolution of $\sim 1\,cm^{-1}$. The temperature dependence of the magnetic susceptibility for single-crystal samples was measured in the temperature range between 2 and 300 K by using a SQUID magnetometer (Quantum Design, MPMS-5S).

3. Results and discussions

Besides yttrium, other rare-earth elements from Gd to Lu can all form the same structure by the solid state reaction method. The mixture of REB_4 (REB_6), amorphous B, SiB_6 and Si with nominal composition of $REB_{20-25}Si_{5-7}$ was first well mixed and pressed into a cylinder by hydrostatic pressure. After being reacted in vacuum at a temperature of 1650°C for 8–12 h, the new phase was produced. In order to suppress the formation of REB_{50}-type compounds, addition of an excess amount of Si in the starting material is essential. In some cases, the powders need to be purified by conc. nitric acid to remove REB_n ($n = 4, 6$) and/or a mixture of HF and HNO_3 to remove the excess Si. Their X-ray diffraction patterns are shown in Fig. 1. The similarity of the powder X-ray profiles between Y and other rare-earth systems indicated that all of them are isomorphous with the compound of $YB_{17.6}Si_{4.6}$. All reflections of these compounds could be indexed with a hexagonal structure. The unit cell parameters and cell volumes, which were indexed with the first 20 reflections, are plotted in Fig. 2a and b, respectively. The cell parameters in Fig. 2a show an interesting staggering pattern, the rare-earth ions with an even number of *f*-electrons (Tb, Ho, Tm) have a larger *a*-axis and smaller *c*-axis than the rare-earth ions with an odd number of *f*-electrons (Gd, Dy and Er). We are not sure if it has any relation with the different states of outside *f*-electrons in the rare-earth elements. However, the cell

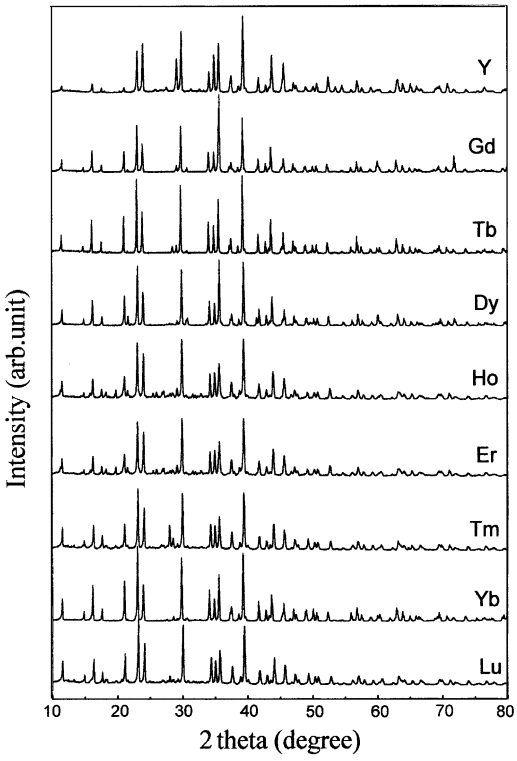

Fig. 1. Powder XRD patterns of $RE_{1-x}B_{12}Si_{3.3-\delta}$ compounds (RE = Y, Gd–Lu). The weak peak around 28° in the systems containing Ho, Er and Tm is attributed to the impurity phase of $REB_{41}Si$.

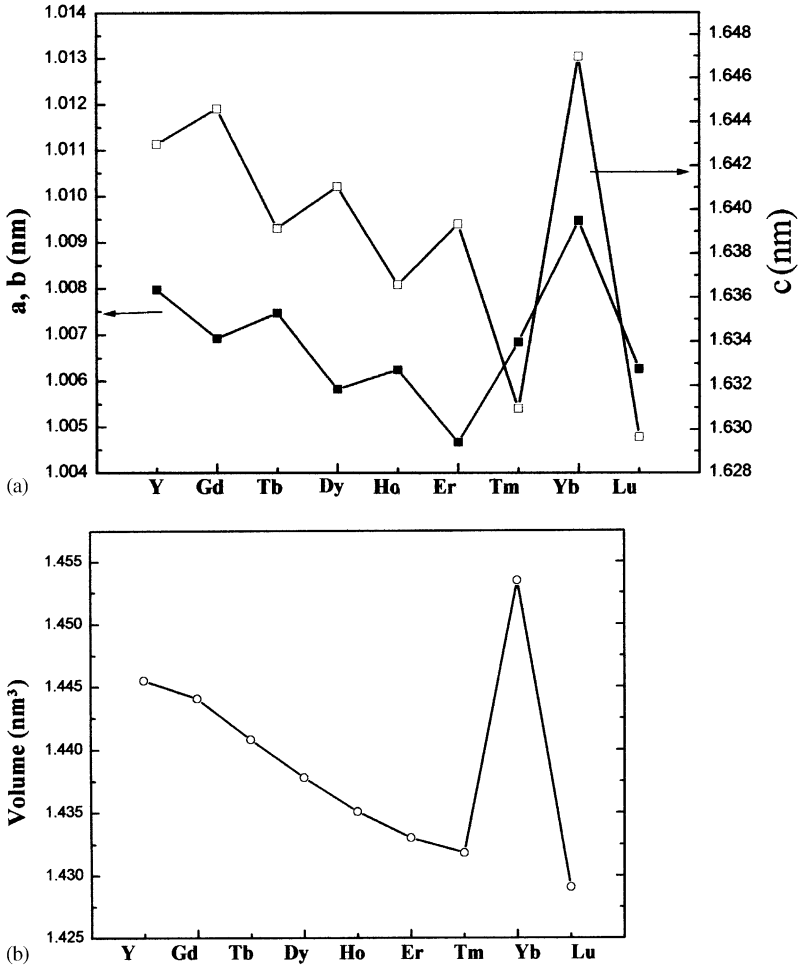

Fig. 2. Indexed parameters of unit cell and volumes for $RE_{1-x}B_{12}Si_{3.3-\delta}$ compounds (RE = Y, Gd–Lu): (a) unit cell parameters of a, b and c; (b) cell volume.

volume is proportional to the ionic radius of trivalent ions of rare-earth elements and they decrease from Gd to Lu with an exception of Yb. The same phenomena were also observed in the compounds of REB_2, REB_4, REB_6, REB_{12} and REB_{66} [17].

In order to have a comparison with the structure of $YB_{17.6}Si_{4.6}$ (or $Y_{0.68}B_{12}Si_{3.01}$), which was solved from single-crystal X-ray reflection data, here we use the X-ray diffraction data from high-quality powder samples of Tb–B–Si system as a representative to analyze their structure. Eight atomic positions were derived from the reflection data by a direct method. According to the height, they are assigned with one Tb, three Si and four B atoms. The atomic positions and the occupancy of atoms Tb and Si3 were further refined with the least square method. The refined atomic positions, thermal factors and occupancies for all elements are listed in Table 1. The fitting of the powder pattern of Tb–B–Si system after final Rietveld refinement is shown in Fig. 3. Thirty-three parameters were refined from 685 diffraction peaks, which gave the fitting results of $R_{wp} = 14.7\%$. Besides the single-crystal data, only 3 silicon positions could be derived from the powder XRD file. The position of Si3 here is split into two in the single-crystal structure analysis [12]. In fact, one of the split positions can also be occupied with B from the bonding environment. Structure analysis

Table 1
Refined atomic positions, thermal factors and occupancies for $Tb_{0.68}B_{12}Si_{3.04}$ from powder X-ray diffraction file

Atom	x/a	y/b	z/c	B (Å^{-2})	Occu.
Tb	2/3	5/6	1/3	1.42(2)	0.68(4)
Si1	1/3	2/3	0.2381(1)	1.56(1)	1.0
Si2	0.4647(6)	0.5352(3)	0.2719(1)	1.56(1)	1.0
Si3	2/3	1/3	0.3815(1)	2.63(5)	0.71(4)
B1	0.4776(3)	0.5223(7)	0.3981(6)	0.74(6)	1.0
B2	0.5097(1)	0.6679(5)	0.4713(6)	0.74(6)	1.0
B3	0.5772(2)	0.4227(9)	0.4382(6)	0.74(6)	1.0
B4	0.6543(3)	0.6232(1)	0.4512(6)	0.74(6)	1.0

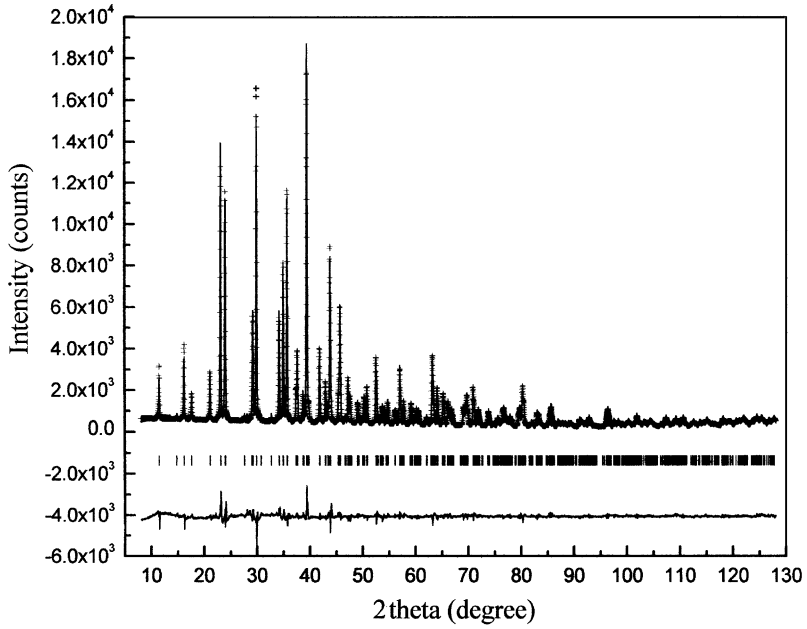

Fig. 3. Rietveld refinement results for $Tb_{0.68}B_{12}Si_{3.04}$ powders synthesized by solid state reaction method. The conventional Rietveld *R*-factors for the pattern are: $R_{wp} = 14.7\%$, $R_{exp} = 8.11\%$, $R_F = 6.37\%$ and $\chi^2 = 3.26$ in the 2θ range of 5–130° with step width of 0.02°.

from powder pattern cannot give such details and the occupancy rate for Si3 equals the total occupancy rate of the two split positions. The occupancies of Tb and Si3 are not full, only 0.684 and 0.714, respectively. The occupancies of rare-earth elements in all recently found compounds are not full [3,5,6,8,12] except for the case of $YB_{41}Si_{1.2}$ [18], so the partial occupancy of rare-earth elements seems to be a quite common character in rare-earth boron-rich compounds. The unusual short bonding distances between Si3–Si3 (1.5824 Å) and Si3–B (average 1.8185 Å) indicate that the partial occupancy for Si3 site is reasonable. The refined composition of $Tb_{0.68}B_{12}Si_{3.04}$ is quite consistent with the chemical analysis and is also very close to that in YBSi system ($Y_{0.68}B_{12}Si_{3.01}$).

Very recently, Salvador et al. [19] have obtained single crystals in the quarternary system of TbBSiC by high-temperature solution growth method with liquid gallium flux. The crystals seem to have the same structure as with our sample. They have indexed the Si3 position here with carbon. In our experiments, it is possible for carbon contamination from the crucible, however, we have neither found any detectible carbon in powders by chemical analysis nor in single crystals by EPMA analysis. In the refinement of single-crystal X-ray data, if we set Si3 position as C, its occupancy is much larger than 1. In addition, the atomic distance between Si3 position and B atoms in the icosahedral in our sample is 1.8185 Å and larger than the normal B–C bonding length. Of course, we believe the Si3 position is the most reasonable position for C if it is incorperated in the samples. So it may be possible that both *RE*–B–Si ternary and *RE*–B–Si–C quarternary systems can form the same structural crystals.

The structure of the powder samples was also investigated by high-resolution transmission microscope (HRTEM). Fig. 4 shows the HRTEM image of the $Tb_{0.68}B_{12}Si_{3.04}$ compound with projection along [001] axis and [211] axis, respectively. The inserted pictures are the corresponding electron diffraction patterns and simulated high-resolution images calculated with Mac-Tempas simulation package based on the multi-slice calculation method. The electron diffraction analysis verified the rhombohedral unit cell. The dark spots with a light center in the high-resolution images are attributed to boron icosahedra. The alignment of boron icosahedra and rare-earth atoms for the structure projected along the [112] direction is quite regular (Fig. 5). The interconnected boron icosahedra form in rhombus and one rare-earth atom resides in the center. The inserted simulation of HRTEM pictures based on the above model match the observed images quite well.

It is interesting to grow bulk single crystals by the floating zone method or other methods in order to measure their physical properties accurately. From the powder synthesis experience, we know that extra silicon can greatly reduce the formation of REB_{50}-type phase. This suggests that additional Si in the feed rods may suppress the nucleation of REB_{50}-type crystal. However, crystal growth by the floating zone method from a feed rod with composition of $YB_{20}Si_{10}$ failed. All the grown crystals were mixtures of YB_{50}(Si) crystals and Si. Further high-temperature heating of powder samples revealed that the above structure was not stable at very

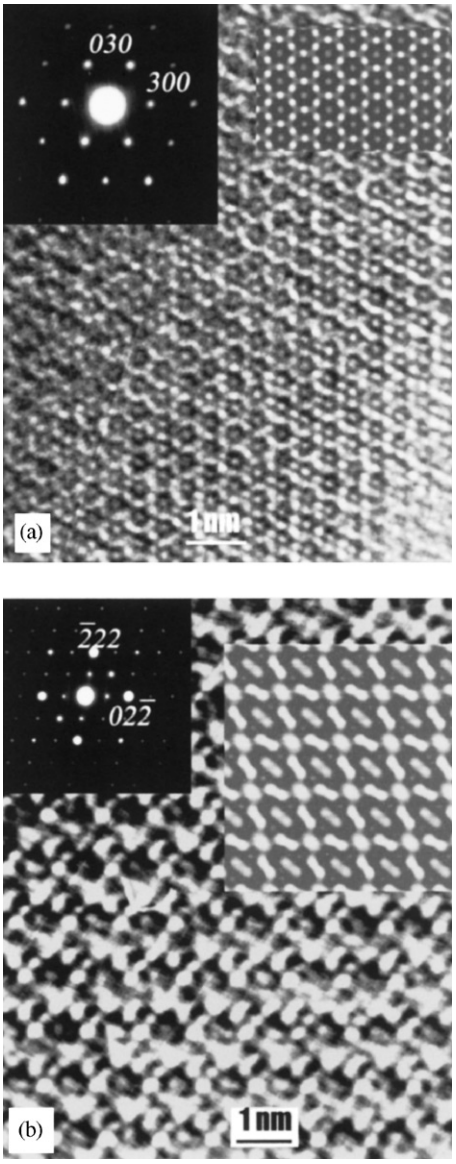

Fig. 4. HRTEM image of $Tb_{0.68}B_{12}Si_{3.04}$ compound: (a) projection along [001] axis; (b) projection along [211] axis.

high temperature and decomposed before melting. Fortunately, single crystals of this structure could be easily grown by high-temperature solution growth method with silicon as the flux. The starting composition for crystal growth was $REB_{20}Si_{50-100}$ and the growth process was performed in a BN crucible. After keeping at about 1600°C for 10 h, the max dimension of single crystals can reach 5 mm at a cooling rate of around 40°C/h. This indicates that the growth rate for the crystal by this method is quite high. Fig. 6 shows the optical microscope images of the single crystals grown with the high-temperature solution method.

The vibrational properties of the crystals were investigated with a micro Raman spectrometer coupled with a metallographic microscope. The scattering data

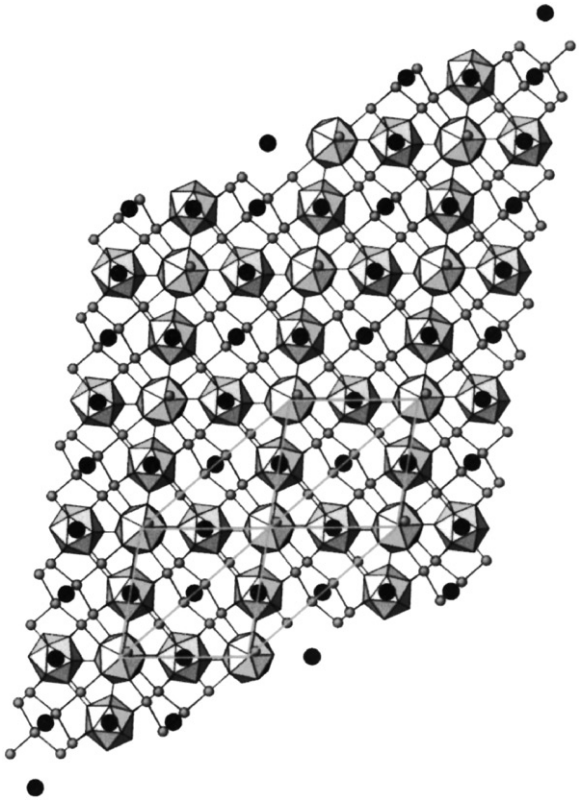

Fig. 5. Schematic crystal structure of $RE_{1-x}B_{12}Si_{3.3-\delta}$ projected along the [211] direction.

were collected by back-scattering geometry and excited by an argon-ion laser operated at a wave length of 514 nm and a low incident power (50 mW) in order to avoid thermal effects. Fig. 7 shows the typical Raman spectrum for $Y_{0.68}B_{12}Si_3$ and $Tb_{0.68}B_{12}Si_3$ crystals. Crystals for all other rare-earth elements showed a similar Raman spectrum. The vibrational frequency dependence on the atomic mass of rare-earth elements can easily derive that the low frequency Raman shifts ($154\,cm^{-1}$ for $Y_{0.68}B_{12}Si_3$ and around $120\,cm^{-1}$ for other rare-earth systems) are contributed by heavy rare-earth atoms. The Raman peaks between 600–1300 cm^{-1} with a wide width may be due to the contribution of various modes of the boron clusters just like the case in boron carbide [20]. The peak around $200\,cm^{-1}$ is very sharp and only with a slight shift for all the crystals. The environment for Si1 and Si2 atoms in this structure is similar to that in diamond-like Si where the strongest Raman shift is around $500\,cm^{-1}$. So the sharp peak at $201 \pm 3\,cm^{-1}$ may be only attributed to the above Si–Si bonds and other peaks between 200 to $600\,cm^{-1}$ may be contributed by other Si–Si bonds and Si–B bonds. The strong intensity of Raman shifts indicates the covalent bonding character for these boron-rich compounds and full index of the vibrational modes is quite difficult and can form another topic.

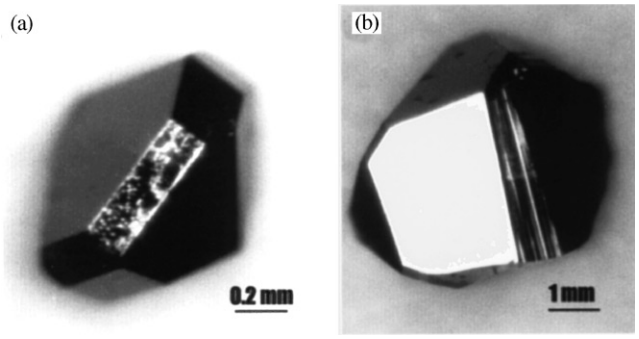

Fig. 6. Optical microscope image of single crystals of $RE_{1-x}B_{12}Si_{3.3-\delta}$ (a) $Y_{0.68}B_{12}Si_3$ crystal and (b) $Tb_{0.68}B_{12}Si_3$ crystal.

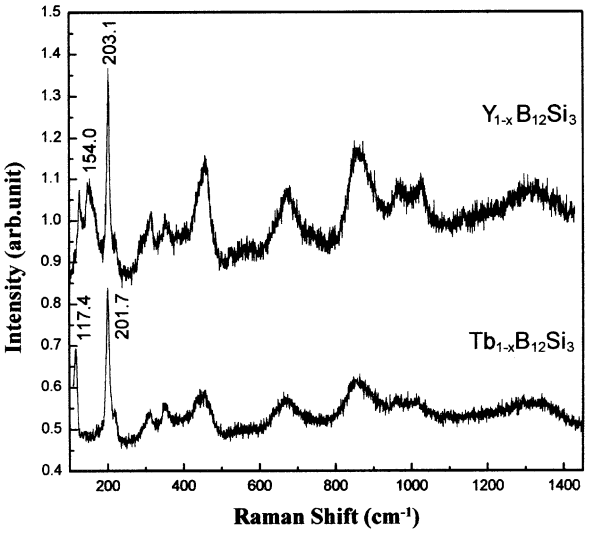

Fig. 7. Raman spectrum of $RE_{1-x}B_{12}Si_{3.3-\delta}$ (RE = Y and Tb). The spectra of other rare-earth compounds are similar with that of $Tb_{0.68}B_{12}Si_{3.04}$.

The temperature dependence of magnetic susceptibility was measured by SQUID and Fig. 8 shows the magnetic susceptibility curves versus temperature for some of the compounds from room temperature down to 2 K. The increase of susceptibility at low temperature range revealed that these compounds are all paramagnetic materials. The behavior of the Ho, Er, and Yb phases (not shown) were similar to the others and are also paramagnetic. The effective magnetic moment for example for the Tb and Dy phases was determined from the high temperature Curie–Weiss fit and yielded 9.2 μ_B/Tb atom and 10.3 μ_B/Dy atom which is slightly smaller than but close to that of the trivalent ions. The indication is that the rare-earth atoms in these phases are trivalent and that the stoichiometry of 0.68 for the rare-earth atoms is possibly smaller than but close to that determined from the structure analysis.

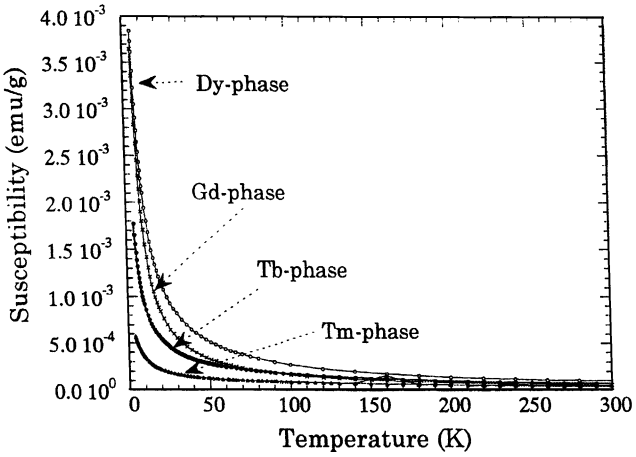

Fig. 8. Temperature dependence of the static magnetic susceptibility of $RE_{1-x}B_{12}Si_{3.3-\delta}$ single crystal (RE = Gd, Tb, Dy and Tm). Other rare-earth elements Ho, Er, Yb and Lu show a similar behavior in susceptibility.

4. Conclusion

A series of new compounds was synthesized by the solid state reaction method in RE–B–Si (RE = Y, Gd–Lu) systems and their crystals were grown by high-temperature solution method with Si flux. The structure was analyzed from powder X-ray diffraction data and high-resolution transmission microscope observation. Their vibrational properties were investigated by Raman scattering and magnetic susceptibility measurement revealed that they were paramagnetic materials.

References

[1] D. Emin, Phys. Today (1987) 55.
[2] P. Rogl, Phase Diagram of Ternary Metal–Boron–Carbon Systems, ASM International, Materials Park, OH, 1998.
[3] T. Tanaka, S. Okada, Y. Yu, Y. Ishizawa, J. Solid State Chem. 133 (1997) 122.
[4] T. Tanaka, S. Okada, Y. Ishizawa, J. Alloys Compd. 205 (1994) 281.
[5] A. Leithe-Jasper, L. Bourgeois, Y. Michiue, Y. Shi, T. Tanaka, J. Solid State Chem. 154 (2000) 130.
[6] F.X. Zhang, A. Leithe-Jasper, J. Xu, T. Mori, Y. Matsui, T. Tanaka, J. Solid State Chem. 159 (2001) 174.
[7] F.X. Zhang, F.F. Xu, A. Leithe-Jasper, T. Mori, T. Tanaka, J. Xu, A. Sato, Y. Bando, Y. Matsui, Inorg. Chem. 40 (27) (2001) 6948.
[8] F.X. Zhang, F.F. Xu, A. Leithe-Jasper, T. Mori, T. Tanaka, A. Sato, P. Salamakha, Y. Bando, J. Alloys Compd. 337 (2002) 120.
[9] W.G. Moffatt, The Handbook of Binary Phase Diagrams, Vol. 1, Genium Publishing Corperation, New York, 1984.
[10] T. Tanaka, S. Okada, Y. Ishizawa, J. Solid State Chem. 133 (1997) 55.
[11] T. Mori, T. Tanaka, IEEE Trans. Magn. 37 (2001) 2144.
[12] F.X. Zhang, A. Sato, T. Tanaka, J. Solid State Chem. 164 (2002) 361.

[13] P.-E. Werner, L. Eriksson, M. Westdahl, J. Appl. Crystallogr. 18 (1985) 367.
[14] A. Altomare, M.C. Burla, G. Cascarano, C. Giacovazzo, A. Guagliardi, A.G.G. Moliterni, G. Polidori, J. Appl. Crystallogr. 28 (1995) 842.
[15] A. Altomare, G. Cascarano, C. Giacovazzo, A. Guagliardi, M.C. Burla, G. Polidori, M. Camalli, J. Appl. Cryst. 27 (1994) 435.
[16] J. Rodrguez-Carvajal, FULLPROF, version 1.7a, 2000.
[17] K.E. Spear, Phase Diagrams, Vol. IV, Academic Press, New York, 1976, p. 120.
[18] I. Higashi, T. Tanaka, K. Kobayashi, Y. Ishizawa, M. Takami, J. Solid State Chem. 133 (1997) 11.
[19] J.R. Salvador, D. Bilc, S.D. Mahanti, M.G. Kanatzidis, Angew. Chem. Int. Ed. 41 (2002) 844.
[20] D.R. Tallant, T.L. Aselage, A.N. Campbell, D. Emin, Phys. Rev. B 40 (1989) 5649.